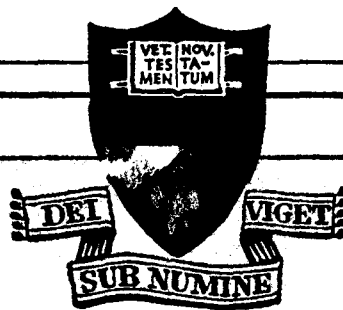
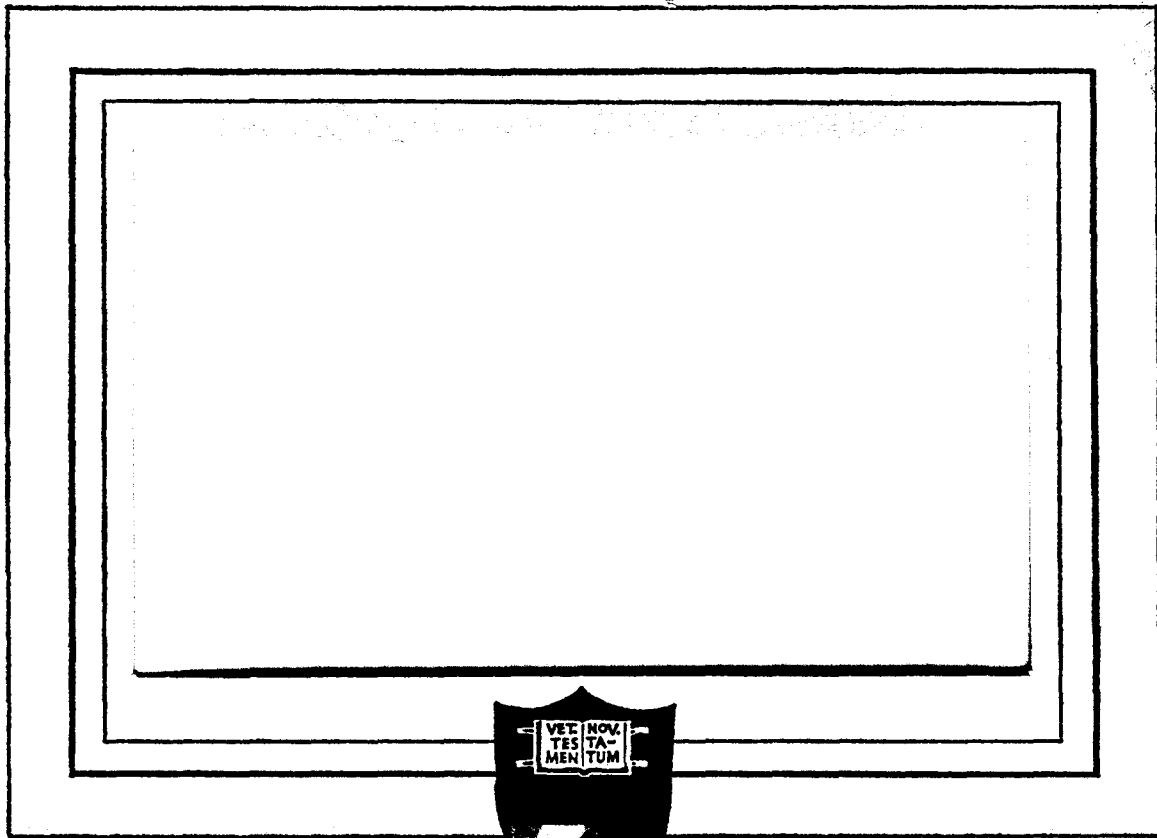


50-5472



FACILITY FORM 802	<b>X67-18146</b>	
	(ACCESSION NUMBER)	(THRU)
	<b>26</b>	<b>21</b>
	(PAGES)	(CODE)
	<b>CR-84395</b>	<b>33</b>
	(NASA CR OR TMX OR AD NUMBER)	(CATEGORY)

PRINCETON UNIVERSITY  
DEPARTMENT OF  
AEROSPACE AND MECHANICAL SCIENCES

U. S. Government Agencies and  
Contractors Only

(NASA-CR-84395) PRE-IGNITION AND IGNITION  
PROCESSES OF METALS Quarterly Progress  
Report, 1 Aug. - 31 Oct. 1966 A.M. Mellor  
(Princeton Univ.) 1 Nov. 1966 26 p

N72-75438

00/99 42976  
Unclas

Second Quarterly Progress Report  
To The  
National Aeronautics and Space Administration  
On NASA Grant NSG-641

on  
PRE-IGNITION AND IGNITION PROCESSES OF METALS  
1 August to 31 October 1966  
Report No. 786

Prepared by:

*Arthur M. Mellor*  
Arthur M. Mellor  
Assistant-in-Research

Approved by:

*James G. Hansel*  
James G. Hansel  
Research Staff Member

1 November 1966

Guggenheim Laboratories for the Aerospace Propulsion Sciences  
Department of Aerospace and Mechanical Sciences  
PRINCETON UNIVERSITY  
Princeton, New Jersey

REPRODUCED BY  
NATIONAL TECHNICAL  
INFORMATION SERVICE  
U.S. DEPARTMENT OF COMMERCE  
SPRINGFIELD, VA. 22161

## I. INTRODUCTION

This report is the Second Quarterly Progress Report to the National Aeronautics and Space Administration by Princeton University on NASA Grant NsG-641, Pre-Ignition and Ignition Processes of Metals, covering the period 1 August to 31 October 1966.

The work reported herein consists of preliminary results on the ignition of magnesium. (See the First Quarterly Progress Report for a discussion of the experimental program under study.) The experiments were performed in the recently acquired induction furnace facility. Induction heating was chosen rather than resistance heating for the investigation for two primary reasons: firstly, because only the load within the work coil is heated during an experiment, heating and cooling rates of several hundred Celsius degrees per minute are attainable; thus furnace down time for cooling is negligible. Secondly, because of the present state of the art in materials, resistance furnaces are limited to temperatures considerably below  $2000^{\circ}\text{C}$ . In induction furnaces, however, again because only the load is heated, much higher temperatures are attainable. Since Al is thought to ignite at about  $2000^{\circ}\text{C}$ , induction heating was the obvious choice for the present investigation.

Section II of the report is a description of the experimental apparatus and procedure. The next section is a discussion of the experimental results obtained thusfar, and the final section of the report is an outline of future research efforts.

## II. INDUCTION FURNACE FACILITY - EXPERIMENTAL APPARATUS AND PROCEDURE

The description of the apparatus is logically divided into four sections: the radio frequency (RF) power supply; the furnace housing and control system; the associated instrumentation; and the materials. The complete facility is shown Fig. 1: the RF generator is shown at the right of the photograph, the pressure vessel housing the work coil and its control panel is at the left, and the instrumentation rack is in the center. Each of these will now be discussed

in turn.

#### A. The RF Generator

The radio frequency power supply in use in this investigation was built by McDowell Electronics, Inc., of Metuchen, New Jersey. Its model number is 10KW-2DFCT/LA and its serial number is 4862. The output power of the unit is continuously variable from 1.2 to 12 KW. Two no load frequency ranges are available: 0.5 to 0.7 and 2.0 to 5.0 Mc/s. For all of the experiments to date, the low frequency side has been used<sup>1</sup>.

This model is equipped with a Leeds and Northrup Speedomax H AZAR (adjustable zero, adjustable range) strip chart potentiometric recorder and Three Action Series 60 Control Unit. When used in the automatic control mode, this control system gives automatic temperature control of  $\pm 0.5^{\circ}\text{C}$  at any chosen preset temperature. For the ignition temperature experiments performed to date, the generator has been used in the manual mode; the control system will be used for the critical temperature experiments to be performed in the near future.

#### B. The Furnace Housing and Control System

The design of the pressure vessel and its control system is based on that of the wire-burning apparatus. A schematic is shown in Fig. 2. The test vessel, inside of which is the work coil, is larger than the vessel comprising the wire-burning apparatus so that a RF current transformer for use with a single turn work coil can be accommodated within the chamber. The cylindrical pressure chamber is of 10 in diameter and 17 in length, or about 1300 cu in volume. The chamber, which is constructed from steel, is lined with a 1/16 in thick aluminum annulus in order to minimize coupling between the chamber and the work coil. Relatively severe coupling occurs in the area of the current feedthroughs in the back of the chamber;

---

<sup>1</sup>The so-called RF skin effect, that is, depth of penetration of heating in the load, is inversely proportional to the output frequency in use. Thus in order to obtain the most uniform sample heating possible, the low frequency RF generator is used.

thus water cooling is used on the outside of the chamber to prevent overheating.

The top of the work coil is mounted in a plane 5 in above the bottom of the chamber; the cylindrical coil is centered 5 in from either side of the chamber and 6 in from the front door. For the experiments to date a  $5\frac{1}{2}$  turn copper coil of  $2\frac{3}{8}$  in inside diameter has been used. In this particular configuration of the work coil, it is aligned with two 1 in diameter quartz windows which are situated 6 in from the front door on the top of the vessel, at  $45^\circ$  from the vertical. Upon one of these windows a Leeds and Northrup Model 8893 Rayotube temperature detector is mounted; the other window is used for visual observation.

The metal sample to be heated is centered in the work coil by a suitable arrangement of fire bricks. Thermocouples mounted within the sample or to the crucible, etc., are connected to the appropriate type of lead wires within the chamber.

Included in the system is a mixing chamber of about 4100 cu in volume. When gas mixtures rather than pure gases are desired for the static test atmosphere, mixing is accomplished in the mixing chamber, which is filled to the desired pressure in the desired proportions. Mixing is accomplished by diffusion.

The schematic shown in Fig. 2 shows a gas dehumidifier in the feed system. It is a Matheson Co. Model 460 Gas Purifier. The cold trap also shown in the schematic is filled with liquid nitrogen for the critical temperature experiments in which the sample is brought to temperature in an inert gas. When this gas is pumped out in order to replace it with the oxidizing gas of interest, the cold trap serves to protect the vacuum pump from any metal vapor entrained in the inert gas.

### C. Instrumentation

The primary data recording unit is a Model FS02W6L Servo/Riter II Potentiometric Strip Chart Recorder built by Texas Instruments, Inc. Two data channels are presently in use for recording the sample temperature as measured by a thermocouple and by the Rayotube.

For the magnesium experiments, chromel-alumel thermocouples with an ice bath reference junction are used; the Model 8893 Rayotube allows blackbody temperature measurements over the range 450 to 1000°C. The Rayotube is protected by a solenoid-actuated shutter which closes automatically whenever a temperature in excess of 1000°C is recorded.

In most experiments performed to date, the metal sample melts before ignition or is in the process of melting at ignition. Thus each chromel-alumel thermocouple is calibrated in situ at the metal melting point (650°C<sup>2</sup>). On this basis, the temperatures reported herein are subject to a maximum error of ± 12°C.

For the experiments to date, the furnace has been controlled manually. In all cases a constant rate of change of sample thermocouple output with respect to time has been attempted. However, because this type of control during the sample heating is somewhat unreproducible, a differentiating circuit which will be used in conjunction with the L & N Series 60 Controller is presently under construction. This unit will allow a more linear rate of change of thermocouple output over the approximate ranges from 20 to several hundred degrees Celsius per minute.

#### D. Materials

As in previous investigations, commercially pure O<sub>2</sub>, CO<sub>2</sub>, and Ar are used. For the magnesium investigation, crucibles of Alundum (predominantly Al<sub>2</sub>O<sub>3</sub>) are used to contain the samples.

The magnesium samples in use to the present time are machined from 15/16 in diam, 99.95% Mg rod. A typical analysis of the rod, supplied by A. D. MacKay, Inc., New York, is shown in Table 1.

The ignition of two different samples sizes, with different surface area to volume ratios (S/V), has been investigated and is discussed in Section III of this report. The first type, of average S/V equal to 0.202 mm<sup>-1</sup>, is designated MGII, MGIV, or MGV, depending on the placement of the sample thermocouple. The dimensions of this type of cylindrical sample are 15/16 in diam by 1½ in length. For the MGII samples, the chromel-alumel thermocouple extends through

---

<sup>2</sup>Kubaschewski, O. and Hopkins, B. E., Oxidation of Metals and Alloys, Butterworths, London, 1962.

the bottom of the crucible and just touches the bottom of the cylindrical sample. For the MGIV samples, a hole is drilled along the centerline of the cylinder, and the thermocouple, encased in ceramic tubing, is mounted  $\frac{1}{4}$  in from the top surface. Finally, for the MGIV samples, the thermocouple is mounted 1 in from the top of the sample on the centerline. In all cases, the bottom edge of the samples is beveled slightly to assure that the bottom surface is in contact with the crucible. The sample dimensions and thermocouple placement are summarized in Table 2.

For purposes of the S/V calculation, it is assumed that the bottom surface of the cylinder is not exposed to the oxidizing gas, and that the reaction surface thus consists only of the side (of  $1\frac{1}{2}$  in length) and the top surface (of  $15/16$  in diam) of the cylinder. Note that this geometrical surface area is assumed even for cases in which the sample melts before ignition. The volume of the samples is obtained by weighing each sample before an experiment and dividing by the room temperature density of Mg, which is taken as  $1.74 \text{ g/cm}^3$ .<sup>3</sup>

Because of poor thermocouple contact with the sample, very few experiments were performed with the MGII samples. For those cases in which ignition occurs above the metal melting point ( $\text{CO}_2$  containing mixtures), MGIV samples are used, and for those cases in which ignition occurs at or below the metal melting point, MGIV samples are used.

A few experiments were performed with MGIV and MGIV samples in which two Pt/Pt13Rh thermocouples were mounted in the sample, one on the centerline (that is, halfway between the centerline and the outer edge), in order to examine the temperature distribution within the sample. For an MGIV sample in  $\text{O}_2$  at a total pressure of 300 torr heated at an average initial rate of  $61^\circ\text{C/min}$ , a typical discrepancy during heating between the two thermocouples was  $20^\circ\text{C}$ . Both thermocouples indicated ignition simultaneously as the metal sample

---

3

Hodgman, C. D., Editor, Handbook of Chemistry and Physics, 42nd Edition, Chemical Rubber, Cleveland, 1960

was melting, with the center thermocouple recording an ignition temperature of  $641^{\circ}\text{C}$  and the side thermocouple indicating  $643^{\circ}\text{C}$ .

For an MGVI sample in  $\text{CO}_2$  at a total pressure of 300 torr heated at an average initial rate of  $53^{\circ}\text{C}/\text{min}$ , a typical discrepancy during the heating below the metal melting point was  $30^{\circ}\text{C}$ . During the melting of the metal, the maximum discrepancy between the two thermocouples occurred initially and was equal to  $11^{\circ}\text{C}$ . Both thermocouples indicated ignition simultaneously; the centerline value was  $788^{\circ}\text{C}$  and the side value was  $786^{\circ}\text{C}$ . Since the experimental temperature accuracy is at worst  $\pm 12^{\circ}\text{C}$ , mounting the sample thermocouples on the centerline of the samples introduces an error small compared to the maximum experimental error.

The other type of sample investigated to this point is designated MGVI and is a Mg wafer  $1/16$  in thick of  $15/16$  in diam. As has been mentioned, these samples were machined from the rod described in Table 1. Two small holes are drilled through these samples and their crucibles, and the chromel-alumel thermocouples are mounted on the top of the sample surface.

The average  $S/V$  of these samples is  $0.772 \text{ mm}^{-1}$ . Again for purposes of the geometrical surface area calculation, it is assumed that only the top and side of the wafer are exposed to the oxidizing gas.

After machining, all samples were stored in the laboratory for several days before use. Thus, a thin room-temperature coat of  $\text{MgO}$  is present on their surfaces before experimentation. The only sample surface pretreatment was a light wiping, in order to remove dirt and surface oils.

#### E. Experimental Procedure

The sample to be ignited is wiped clean and weighed. It is then placed in its crucible, and the crucible and sample are mounted within the work coil. The sample thermocouple is connected to the appropriate lead wires.

The front door of the chamber is closed and the chamber and feed system is evacuated. After a pressure on the order of one torr is attained in the system, the chamber is filled with the



appropriate oxidizing gas or gas mixture to the desired pressure, directly from the gas cylinder or from the mixing chamber, respectively. The furnace is placed in the manual control mode and the heating is begun.

As soon as ignition has occurred, the furnace is turned off and the pressure vessel is purged with high pressure Ar in order to extinguish the fire as soon as possible. Only one fire has resulted in serious damage to the interior of the chamber. In an experiment at 5 atm of pure  $O_2$ , during the subsequent temperature rise after ignition the crucible melted and molten Mg and/or molten Alundum came in contact with the copper work coil, which ignited and burned to the feedthroughs at the back of the chamber. Since that time, a larger inside diameter coil and a different fire-brick arrangement have prevented a recurrence of this accident.

After the Mg fire is extinguished, the chamber is exhausted to 1 atm and opened. The sample, crucible, and thermocouple are removed.

Experiments are performed in pure  $O_2$ , pure  $CO_2$ , and 50%-50% mixtures of  $O_2$ - $CO_2$ ,  $O_2$ -Ar, and  $CO_2$ -Ar, at total pressures of 50, 100, and 300 torr, and 1, 2, and 5 atm. Except for free convection, the atmospheres are static.

### III. EXPERIMENTAL RESULTS ON THE IGNITION OF MAGNESIUM

Before discussing the experimental results which have been obtained during the report period on the ignition of magnesium, a brief review of the trends expected on the basis of the physical model of metal ignition for variations of the experimental parameters will be given. The model has been discussed in detail in the last three progress reports. The independent experimental variables are gas pressure and composition, metal sample size, and applied heating rate.

The intersection of the  $\dot{q}_{chem}$  and  $\dot{q}_{loss}$  curves which occurs at the critical temperature is in the low temperature regime, in which the reaction rate is kinetically controlled. The pressure dependence of this intersection may be examined as follows:

$$(\dot{q}_{chem})|_{T_s=T_{crit}} = (\dot{q}_{loss})|_{T_s=T_{crit}} \quad (1)$$

$$\dot{q}_{chem} = \dot{m}Q_{chem} = a(T_s)p_{ox}^n \quad (2)$$

$$\dot{q}_{loss} = \dot{q}_{cond,f} + \dot{q}_{rad} + \dot{q}_{cond,g} \quad (3)$$

$$= b'(T_s) + c(T_s)p_{tot}^m = b'(T_s) + c(T_s)(p_{dil} + p_{ox})^m \quad (4)$$

$$= b(T_s) + c(T_s)p_{ox}^m \quad (5)$$

$$\therefore a(T_{crit})p_{ox}^n = b(T_{crit}) + c(T_{crit})p_{ox}^m \quad (6)$$

where it has been assumed that the radiation heat loss,  $\dot{q}_{rad}$ , is independent of gas pressure, and where

$\dot{m}$  = chemical reaction rate, mole fuel/cm<sup>2</sup>sec;

$Q_{chem}$  = chemical energy release, cal/mole fuel;

$a(T)$ ,  $b'(T)$ ,  $b(T)$ , and  $c(T)$  = functions of temperature independent of pressure, cal/cm<sup>2</sup>sec torr<sup>n</sup>, cal/cm<sup>2</sup>sec, cal/cm<sup>2</sup>sec, and cal/cm<sup>2</sup>sec torr<sup>m</sup>, respectively;

$T_s$  = metal surface temperature, °K;

$\dot{q}_{cond,i}$  = conduction heat loss into the fuel (f) or gas (g), cal/cm<sup>2</sup>sec;

$p_i$  = total pressure (tot), or partial pressure of oxidizer (ox) or diluent (dil), torr;

$n$  and  $m$  = pressure dependence exponents, dimensionless.

The complicated nature of the coefficients  $a$ ,  $b$ , and  $c$ , and the uncertainty in the numerical values of the parameters which they involve preclude any further progress with Eqn. (6). However, the pressure dependence of the ignition temperature may be examined.

Ignition is said to occur when the magnitude of  $(\dot{q}_{chem} - \dot{q}_{loss})$  attains its maximum value above the critical temperature:

$$(\dot{q}_{chem} - \dot{q}_{loss})|_{T_s = T_{ign}} = \text{maximum} \quad (7)$$

$$\therefore \left( \frac{\partial \dot{q}_{chem}}{\partial T_s} - \frac{\partial \dot{q}_{loss}}{\partial T_s} \right) \Big|_{T_s = T_{ign}} = 0 \quad (8)$$

$$\left( \frac{\partial \dot{q}_{chem}}{\partial T_s} \right) \Big|_{T_s = T_{ign}} = \left( \frac{\partial \dot{q}_{loss}}{\partial T_s} \right) \Big|_{T_s = T_{ign}} \quad (9)$$

$$\left( \frac{\partial \dot{q}_{chem}}{\partial T_s} \right) = \frac{\partial a}{\partial T_s} P_{ox}^n = A(T_s) P_{ox}^n \quad (10)$$

$$\left( \frac{\partial \dot{q}_{loss}}{\partial T_s} \right) = \frac{\partial b}{\partial T_s} + \frac{\partial c}{\partial T_s} P_{ox}^m = B(T_s) + C(T_s) P_{ox}^m \quad (11)$$

$$\therefore A(T_{ign}) P_{ox}^n = B(T_{ign}) + C(T_{ign}) P_{ox}^m \quad (12)$$

where  $A(T_s)$ ,  $B(T_s)$  and  $C(T_s)$  = functions of temperature independent of pressure,  $\text{cal/cm}^2 \text{sec}^\circ \text{K torr}^n$ ,  $\text{cal/cm}^2 \text{sec}^\circ \text{K}$ , and  $\text{cal/cm}^2 \text{sec}^\circ \text{K torr}^m$  respectively.

Again,  $A$ ,  $B$ , and  $C$  cannot be calculated, but by comparison of Eqns. (6) and (12) one sees that in any case the pressure dependence of the critical and ignition temperatures will be similar.

The pressure dependence of the transition temperature is available only from examination of the pertinent literature on the oxidation of the particular metal-oxidizer system.

One would expect, however, that if mechanical stress cracking occurred at a critical oxide thickness, the transition temperature would decrease with increasing oxidizer pressure, since the reaction rate increases with pressure.

Other than oxidizer pressure and mole fraction, a second independent variable in the experiment is the metal sample size, or more precisely, the surface area to volume ratio ( $S/V$ ) of the sample. It has been shown in previous reports that the critical temperature decreases with decreasing sample size (increasing  $S/V$ ), and that therefore the transition temperature, which is assumed independent of size, will become controlling in ignition. Thus in the case of a

metal whose bulk ignition is controlled by its critical temperature, as Mg in  $O_2$ ,<sup>4</sup> as the sample size is decreased, the ignition temperature will decrease accordingly to the transition temperature.

The dependence of transition temperature on applied furnace heating rate is easily examined intuitively. Since the transition temperature is in most cases estimated from isothermal oxidation experiments, in which equilibrium is established, these temperatures are expected to be upper limiting values, that is, for the case of zero heating rate. As the heating rate is increased from zero, it would be expected that the transition temperature will decrease somewhat, although the numerical values involved are unclear as very few non-isothermal oxidation experiments have been reported in the literature. Clearly, however, for the case of heating rates large compared to the chemical heat release due to oxidation, that is, for heating times fast compared with some characteristic oxidation time, the transition temperature will be governed predominantly by any oxide film pre-existing on the metal surface. In the limiting case of zero initial oxide thickness and infinite applied heating rate, the transition temperature is of course zero, but for realistic cases it is impossible to estimate the decrement in transition temperature. It is not felt, however, that the transition temperature will become unimportant in metal ignition for realistic applied heating rates.

The critical temperature dependence on applied furnace heating rate is not clear. If one assumes that the rate of heat loss from the sample surface is independent of the heating rate at any given surface temperature, then the only effect of the heating rate will be to increase the magnitude of the heat input rate ( $\dot{q}_{chem} + \dot{q}_{applied}$ ) at that surface temperature. Under this assumption, because the  $\dot{q}_{input}$  curve is displaced upwards and because the  $\dot{q}_{loss}$  curve remains the same on the  $\dot{q}$  versus surface temperature diagram, the critical temperature intersection will also move to lower temperatures as the applied heating rate is increased. However, in the more realistic case, in which  $\dot{q}_{loss}$  will depend on  $\dot{q}_{applied}$ , the trend is unclear and may go

---

4

See in particular the Third Semi-Annual Progress Report for a discussion of the Mg critical temperature.

in either direction, depending on the relative displacements of the  $\dot{q}_{\text{input}}$  and  $\dot{q}_{\text{loss}}$  curves as functions of applied furnace heating rate.

To reiterate, the important independent experimental variables (for a given metal-oxidizer system) are oxidizer pressure (and mole fraction), sample size, and furnace heating rate. The oxidizer pressure trend of the critical and ignition temperatures is expected to be the same independent of sample size, and for the case of Mg, the ignition temperature is expected to decrease to the limiting value of the transition temperature at that particular pressure as the sample S/V is increased. Discussion of the pressure dependence of the Mg transition temperature will be delayed until the next progress report.

It is expected that the transition temperature will decrease with increasing applied furnace heating rate, and observation of such a trend may indicate that the transition temperature is controlling in ignition. The dependence of critical temperature on heating rate is unclear: an increase in ignition temperature with increasing heating rate may indicate that the critical temperature controls ignition, but the contrary trend sheds no light on the situation.

As was mentioned in Section II of the present report, ignition temperature experiments have been accomplished for Mg samples of two sizes in various oxidizing gases. The experimental results are shown in Fig. 3 and 4 for MGII, MGIV, and MGVI, and MGVI respectively. The results of each ignition temperature experiment are plotted versus total pressure on a logarithmic axis. At least two experiments were performed at each test point, which are listed in Section II. Results are missing in some cases at total pressures of 50 and 100 torr, because arcing occurred between the turns of the work coil before the sample ignited. Occasionally arc-induced ignitions were observed; these data are not included in the Figures. In some cases arcing was observed at room temperature as the heating was started. The heavy solid lines shown in Fig. 3 and 4 are the average ignition temperatures as a function of total pressure in the

various gas compositions, interpolated between the test points.

The average initial heating rate which is given in Fig. 3 and 4 was obtained as follows: in the approximate temperature range from  $50^{\circ}$  to  $200^{\circ}\text{C}$ , the sample thermocouple output was taken as linear over one minute of the heating period. (Recall that this output is kept as linear with respect to time over the entire temperature range of interest as is possible manually.) Such a measurement was made for each experiment. The value reported in the Figures is the average of the individual values for all the experiments performed at a given sample S/V. The influence of heating rate on ignition temperature will be described below.

It is seen from Fig. 3 that for the large Mg cylinders in all the oxidizing gases of interest several well-defined trends are evident. The ignition temperature in  $\text{O}_2$  or  $\text{O}_2\text{-Ar}$  is independent of pressure, a result due to ignition occurring at the metal melting point of  $650^{\circ}\text{C}$ .<sup>2</sup> This result is in agreement with literature values of the ignition temperature, as has been discussed in previous reports. However, most of the values, both in the literature and in the present investigation are somewhat below the metal melting point. It was observed here that the Mg samples began to melt on their outer surface, due to the RF skin effect. Ignition generally occurred in this region, and the subsequent flame spread enveloped the sample. As the center portion of the sample near the thermocouple had not yet melted, the thermocouple registered a somewhat lower ignition temperature. The fact that the ignition temperature of bulk Mg is equal to the metal melting point has not been stressed in the literature.

In  $\text{CO}_2$  containing gases, ignition occurs above the metal melting point, also in agreement with the literature. Furthermore, the ignition temperature is a strong function of pressure. This is not a result of diffusional dependence of the ignition temperature, for if the data are plotted versus the  $\text{CO}_2$  partial pressure rather than versus the total pressure, the  $\text{CO}_2$  and  $\text{CO}_2\text{-Ar}$  results are essentially equivalent, as is shown in Fig. 5. (The average ignition temperature for each test point is shown in Fig. 5.) One notes the inhibiting effect that  $\text{CO}_2$  has upon the  $\text{Mg-O}_2$  ignition.

The ignition temperature of the MGVI wafers in  $O_2$  or  $O_2$ -Ar is also equal to the melting point of the metal, although the results shown in Fig. 4 are somewhat lower than those for the Mg cylinders, as ignition occurred somewhat earlier in the melting process. Considerable scatter is evident in those results obtained in  $CO_2$  containing mixtures, which is a result of the mode of ignition.

In pure  $CO_2$ , 50%  $CO_2$ -50% Ar, or 50%  $O_2$  - 50%  $CO_2$ , during the melting of the metal, occasionally bright white flashes were observed on isolated sections of the sample. In some cases, these flashes lead immediately to flame spread and combustion, but in other cases, predominantly at the lower pressures investigated, ignition did not occur until well after the metal had melted. Since self-sustaining combustion must follow ignition, and since the initial occurrence of the isolated flashes did not always lead to flame, considerably more scatter is observed in the wafer results than in the cylinder results.

The average ignition temperature is plotted versus  $CO_2$  partial pressure in Fig. 6. Again it is seen that the former depends only on the latter value. This pressure dependence exhibited by both sample sizes will be compared to that of the critical temperature, when values of the latter are obtained during the next report period.

A major difference between the pressure dependences of the ignition temperature of the cylinders and wafers is apparent by comparing Fig. 5 and 6. By merely changing the sample size, the ignition temperature has been found to reverse its dependence on pressure: for the cylindrical samples, it increases with pressure, while for the smaller samples, it first increases and then decreases with increasing pressure. This result can be explained by an examination of Eqn. (12).

The term which depends most strongly on sample size is the conduction loss into the fuel, which is included in  $B(T_g)$  in Eqn. (12). It has been shown in previous reports that this heat loss term increases with decreasing size; thus as the latter is decreased, the first term on the right hand side of Eqn. (12) will

overpower the second term, and the major pressure dependence will be that of the left hand side. Examination of the pressure trend of ignition temperature for smaller sample sizes should thus show a uniform decrease in ignition temperature with increasing pressure; these experiments are currently underway. Preliminary results show that this trend is indeed the case.

Results demonstrating the influence of initial heating rate on ignition temperature for the two sample sizes examined to date are shown in Tables 3 and 4 for the cylinders and wafers, respectively. These experiments have been conducted in the various gas combinations only at total pressures of 300 torr and 2 atm. Although in either case any trend is slight, there appears to be a small increase in ignition temperature with increasing applied furnace heating rate. As has been discussed, this trend may indicate that the critical temperature controls the ignition of these two particular sample sizes, a result which is in agreement with the literature on the ignition of magnesium.<sup>4</sup>

Brightness ignition temperatures, as measured by the Rayotube, are given in Tables 3 and 4. In particular, in Table 3 it is noted that there is poor correlation between the thermocouple ignition temperature trends and those of the brightness temperature, which is attributed to several causes: firstly, it is not possible to focus the Rayotube until the target is at a brightness temperature of 450°C; at the low temperatures encountered in the ignition of Mg, focusing is extremely difficult. Furthermore, the placement of the sample in the work coil is critical, and although it is maintained as constant as is possible, slight variations from experiment to experiment give large variations in Rayotube viewing area, and thus brightness temperature. The nature of the metal surface near the ignition event is generally extremely unsmooth, and large oxide pustules are observed to grow in isolated areas. Thus the emissivity of the surface varies from experiment to experiment. For these reasons, little value is placed on the brightness ignition temperatures, and no attempt will be made to calculate a mean emissivity for the sample surface.



Essentially then the main use of the Rayotube has been as a photocell, and the thermocouple ignition temperature as defined by the Rayotube (maximum rate of change of light intensity) may be compared with that defined by the thermocouple itself (maximum rate of change of sample temperature). In all cases examined thusfar any discrepancies have been within the experimental error ( $\pm 12^{\circ}\text{C}$ ) and usually result from the initial flame occurring out of view of the Rayotube.

Observation of the combustion of both sizes of Mg samples has been cursory because it is desirable to extinguish the fires as soon as possible after ignition in order to avoid damage to the interior of the test vessel. Generally, however, in  $\text{O}_2$ ,  $\text{O}_2\text{-Ar}$ , and  $\text{O}_2\text{-CO}_2$  mixtures, both types of sample burn with a white flame too brilliant to resolve any structure with the naked eye. In  $\text{CO}_2$  and  $\text{CO}_2\text{-Ar}$  mixtures, the flame is orange-colored and much more dim. Flame-spreading is much slower in this case, and at times several well-developed flamelets occupy the surface. The products of combustion in the  $\text{O}_2$  containing gases are predominantly white, and great quantities of white smoke are produced during the reaction. In the carbonaceous gases much less smoke is produced, and the powdery products found in the crucible contain great amounts of black deposits, probably carbon. In all gas compositions, the brilliance of the flame is observed to increase with increasing total pressure.

To summarize, some of the predictions based on the physical model of metal ignition are apparent in the preliminary results on the ignition of magnesium. It is hoped that these trends will become more clear in the experiments to be performed during the next report period.

#### IV. FUTURE EFFORTS

As has been mentioned, the influence of sample size on the ignition of magnesium will be investigated further. A similar study of the ignition of magnesium in pure nitrogen will be started. During the next report period, the two types of critical temperature

experiments discussed in the last progress report will be accomplished, and it is hoped that the similar investigation of the ignition of aluminum will be started. Experiments with coated Al foils, similar to those performed in the wire-burning apparatus with Al wires, will be conducted upon completion of the Al ignition investigation.

TABLE 1.

TYPICAL ANALYSIS OF 99.95% MAGNESIUM  
ROD, 15/16 in diam

Element	Percent
Al	.0070
Ni	< .0005
Cu	< .0010
Fe	.0010
Mn	.0020
Si	.0060
Ca	.0040
Pb	.0010
Zn	.0100
Ag	< .0005
Na	< .0010

Total impurities less than .0340%. Mg (by difference)  
99.966%.

TABLE 2.

MAGNESIUM SAMPLE DESIGNATIONS

Designa- tion	Average S/V, mm <sup>-1</sup>	Source	Sample Geometry	Sample Dimensions	Thermocouple Position
MGII	0.202	15/16" rod	cylinder	15/16" diam by 1 1/2"	touching bottom
MGIV	0.202	15/16" rod	cylinder	15/16" diam by 1 1/2"	1/4" from top on centerline
MGV	0.202	15/16" rod	cylinder	15/16" diam by 1 1/2"	1" from top on centerline
MGVI	0.772	15/16" rod	wafer	15/16" diam by 1/16"	touching top

TABLE 3.

EFFECT OF HEATING RATE ON IGNITION TEMPERATURE:  
 MGII, MGIV, AND MGVI SAMPLES (AVERAGE S/V = 0.202 mm<sup>-1</sup>)

Gas	Total Pressure	Time Average Initial Heating Rate, °C/min	Ignition Temperature, °C	Brightness Temperature °C
O <sub>2</sub>	300 torr	10	646	---
		77	645	527
		87	647	---
		198	646	---
	2 atm	24	643	---
		74	647	450
		84	645	485
		197	648	---
	50% O <sub>2</sub> - 50% Ar	27	648	---
		89	647	---
		93	649	455
		97	642	---
	2 atm	120	647	---
		22	647	---
		94	648	490
		95	645	---
CO <sub>2</sub>	300 torr	147	645	460
		28	799	480
		61	863	570
		~90	825	650
	2 atm	105	787	545
		32	880	600
		~90	879	650
		92	881	655
	50% CO <sub>2</sub> - 50% Ar	174	896	560
		25	769	540
		82	759	515
		112	776	555
	2 atm	159	817	585
		43	833	550
		~90	874	655
		133	852	630
50% O <sub>2</sub> - 50% CO <sub>2</sub>	300 torr	141	837	590
		36	622	---
		79	700	515
		91	658	450
	2 atm	100	655	---
		143	672	---
		18	730	---
		79	789	515
	50% CO <sub>2</sub>	79	780	470
		96	795	535
		106	801	480

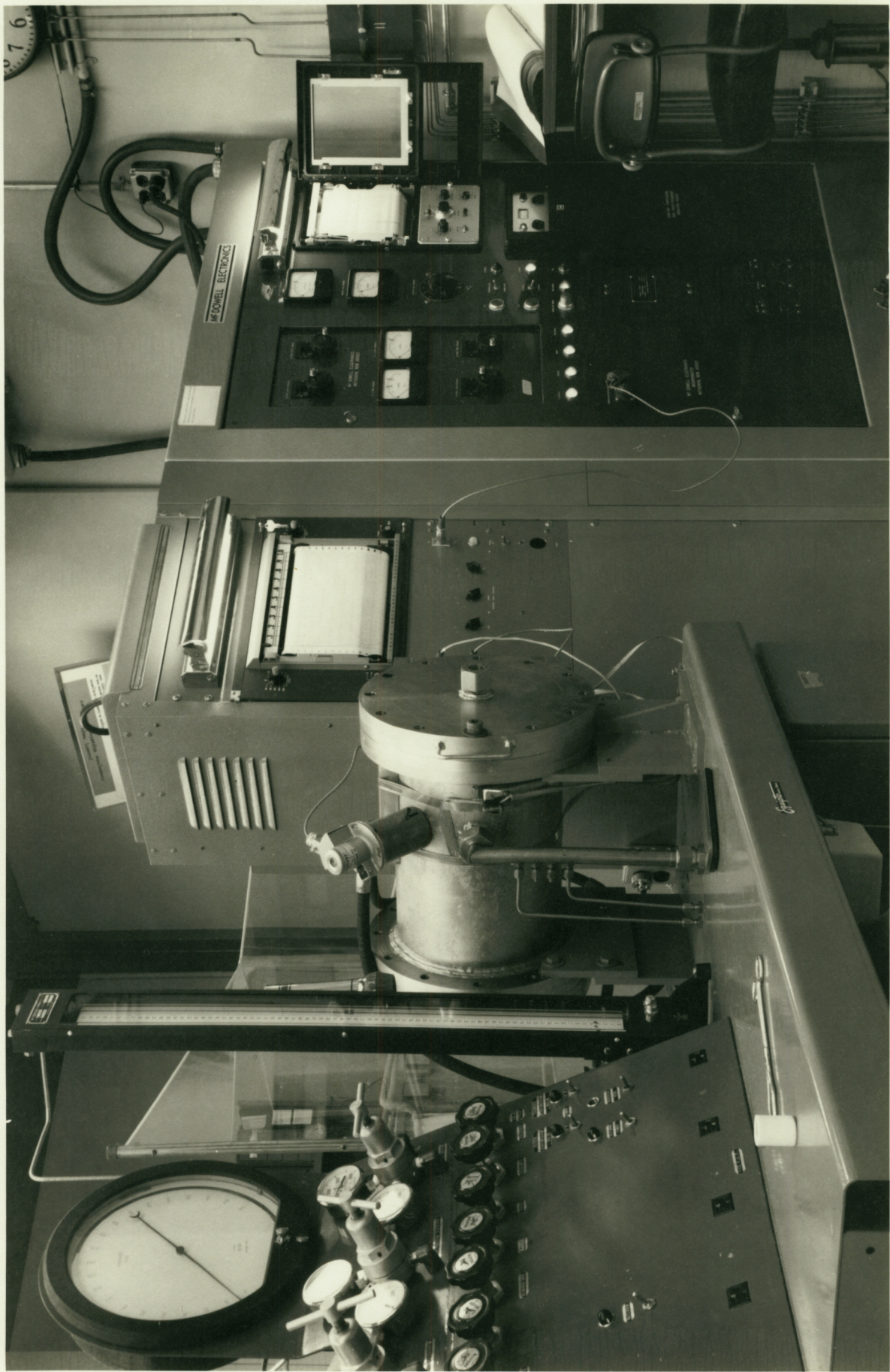
TABLE 4.

EFFECT OF HEATING RATE ON IGNITION TEMPERATURE:

MGVI SAMPLES (AVERAGE S/V = 0.772 mm<sup>-1</sup>)

Gas	Total Pressure	Time Average Heating Rate, °C/min	Initial Ignition Temperature °C	Brightness Temperature °C
O <sub>2</sub>	300 torr	22	606	---
		40	641	---
		71	645	---
		111	630	---
	2 atm	6	661	---
		59	685	---
		63	627	---
		91	636	---
50% O <sub>2</sub> - 50% Ar	300 torr	62	615	---
		66	645	---
		119	641	---
	2 atm	12	630	---
		52	626	---
		69	626	---
		121	640	---
CO <sub>2</sub>	300 torr	11	764	---
		34	798	---
		50	747	---
		87	816	450
	2 atm	18	798	480
		39	607	---
		64	613	---
		152	829	---
50% CO <sub>2</sub> - 50% Ar	300 torr	17	745	---
		51	751	---
		79	748	480
		133	810	---
	2 atm	11	637	---
		76	605	---
		81	825	---
		141	781	---
50% O <sub>2</sub> - 50% CO <sub>2</sub>	300 torr	17	647	---
		47	642	---
		47	637	---
		186	697	---
	2 atm	21	728	---
		48	621	---
		56	621	---
		120	752	---



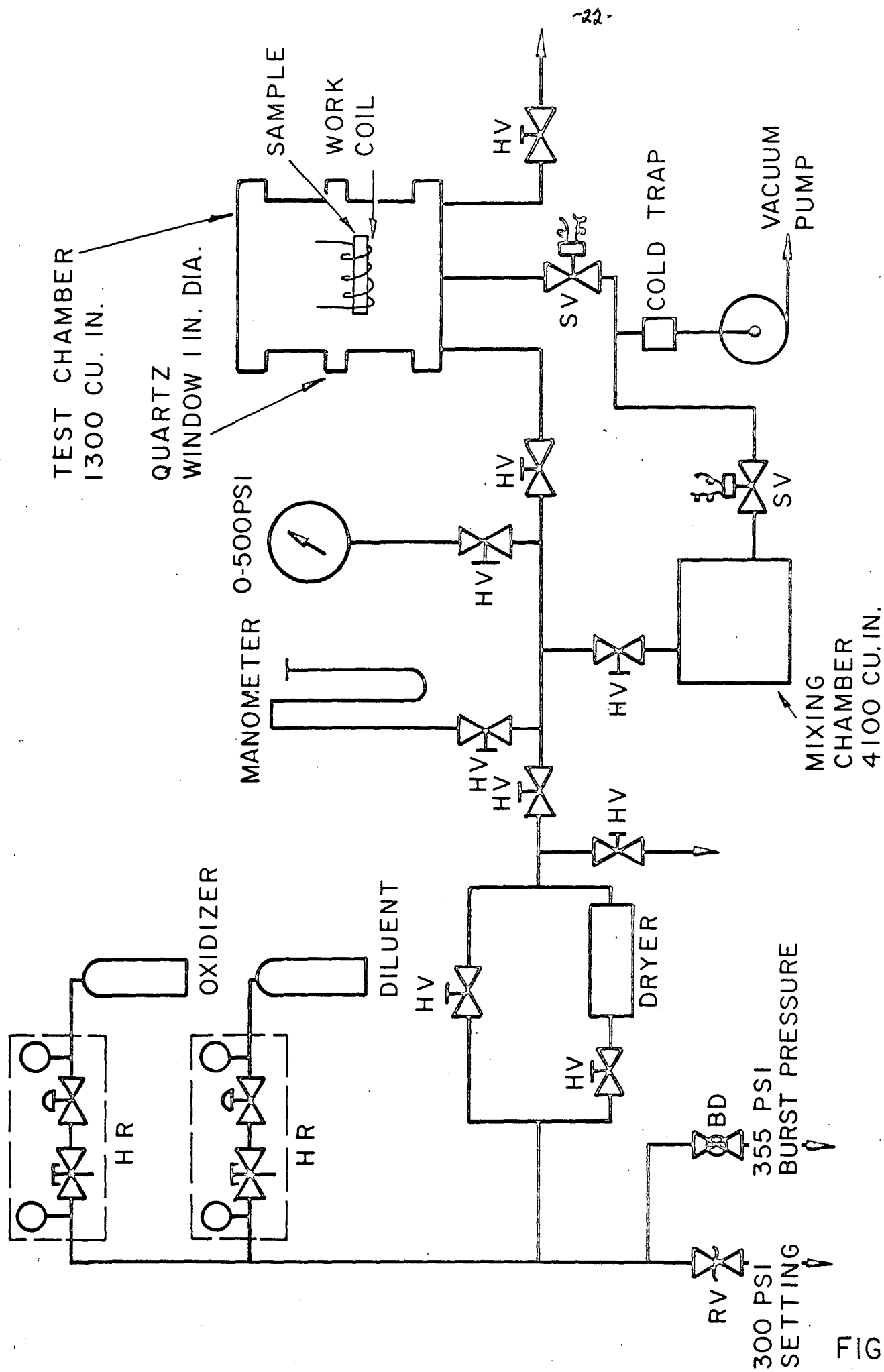


AP24 P-25 66

AP25-P25-66

FIGURE I.



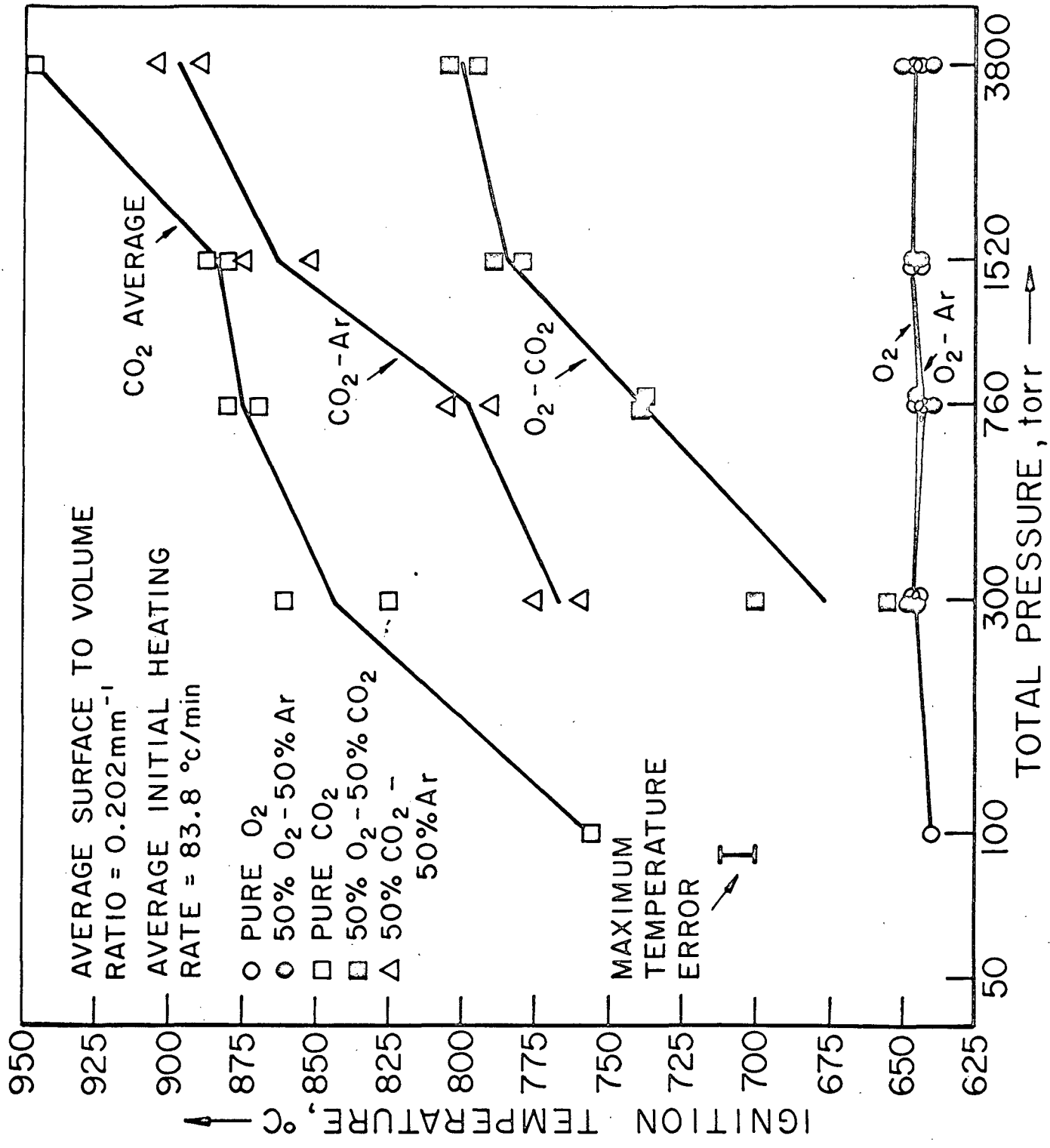


INDUCTION FURNACE FACILITY TEST APPARATUS SCHEMATIC

FIGURE 2

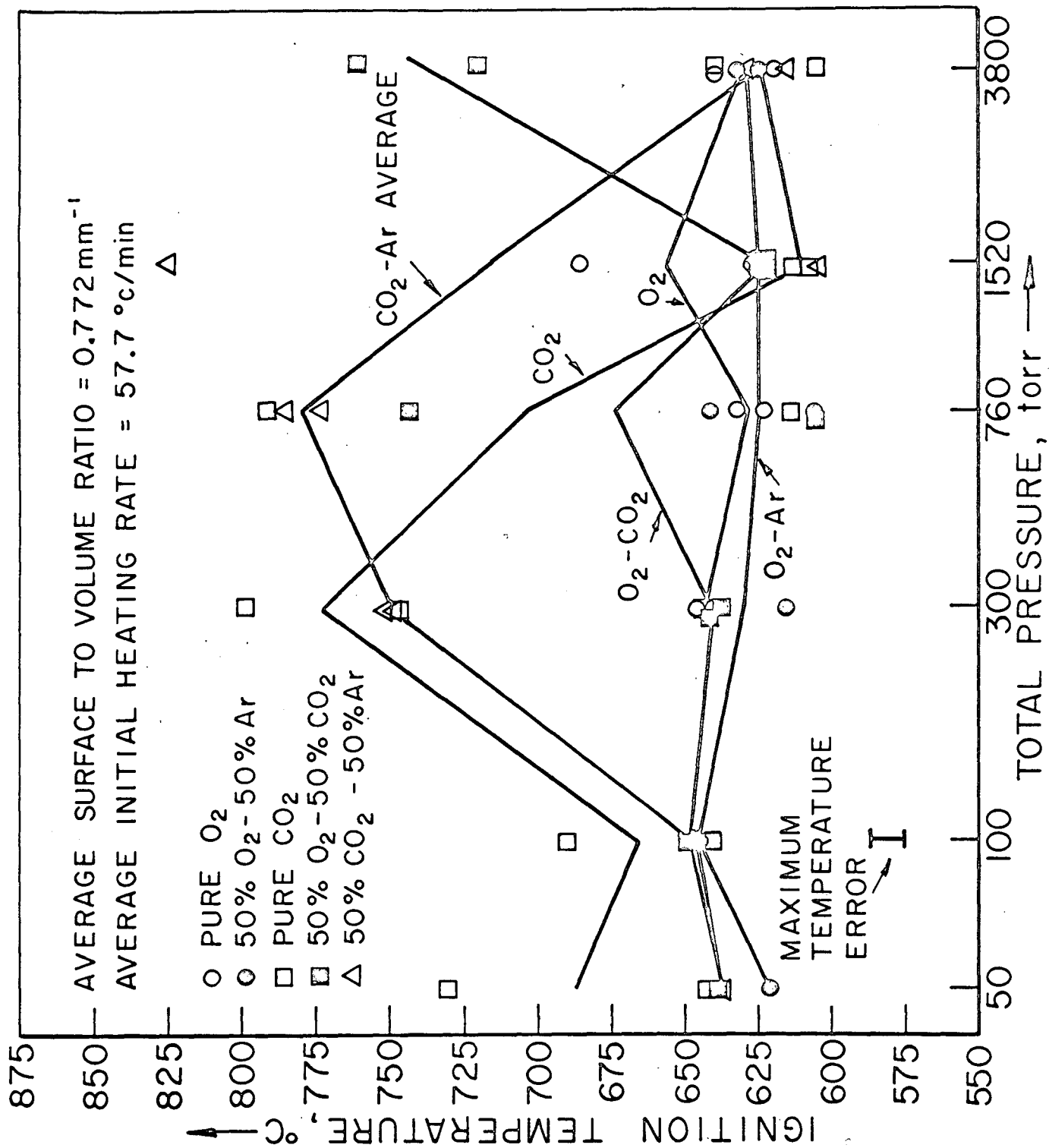


AP29-R4029-66



MAGNESIUM IGNITION TEMPERATURE IN VARIOUS OXIDIZING GASES VS TOTAL PRESSURE (MGII, MGIV, MG V)

FIGURE 3



MAGNESIUM IGNITION TEMPERATURE IN VARIOUS  
 OXIDIZING GASES VS TOTAL PRESSURE (MGVI)

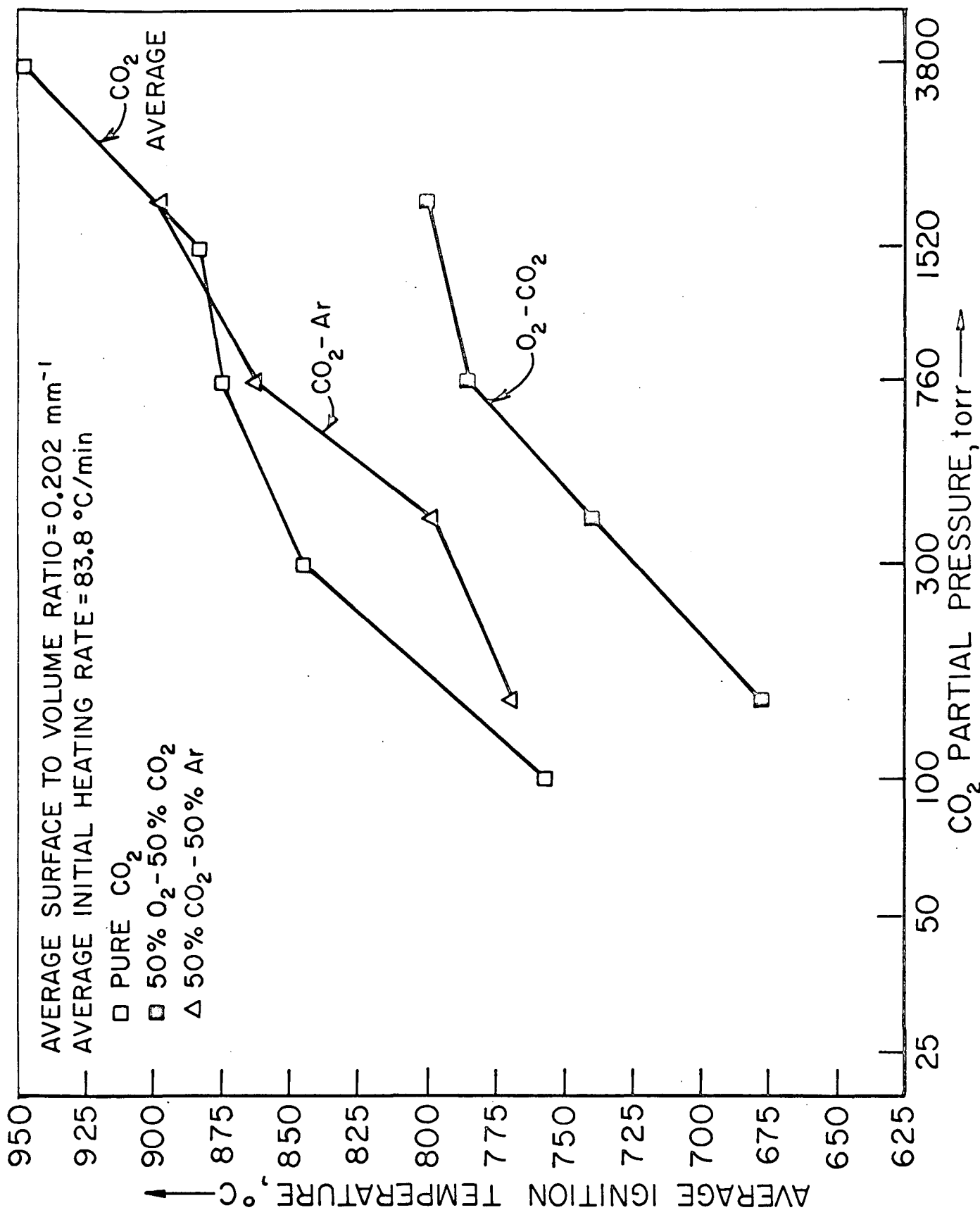


FIGURE 5

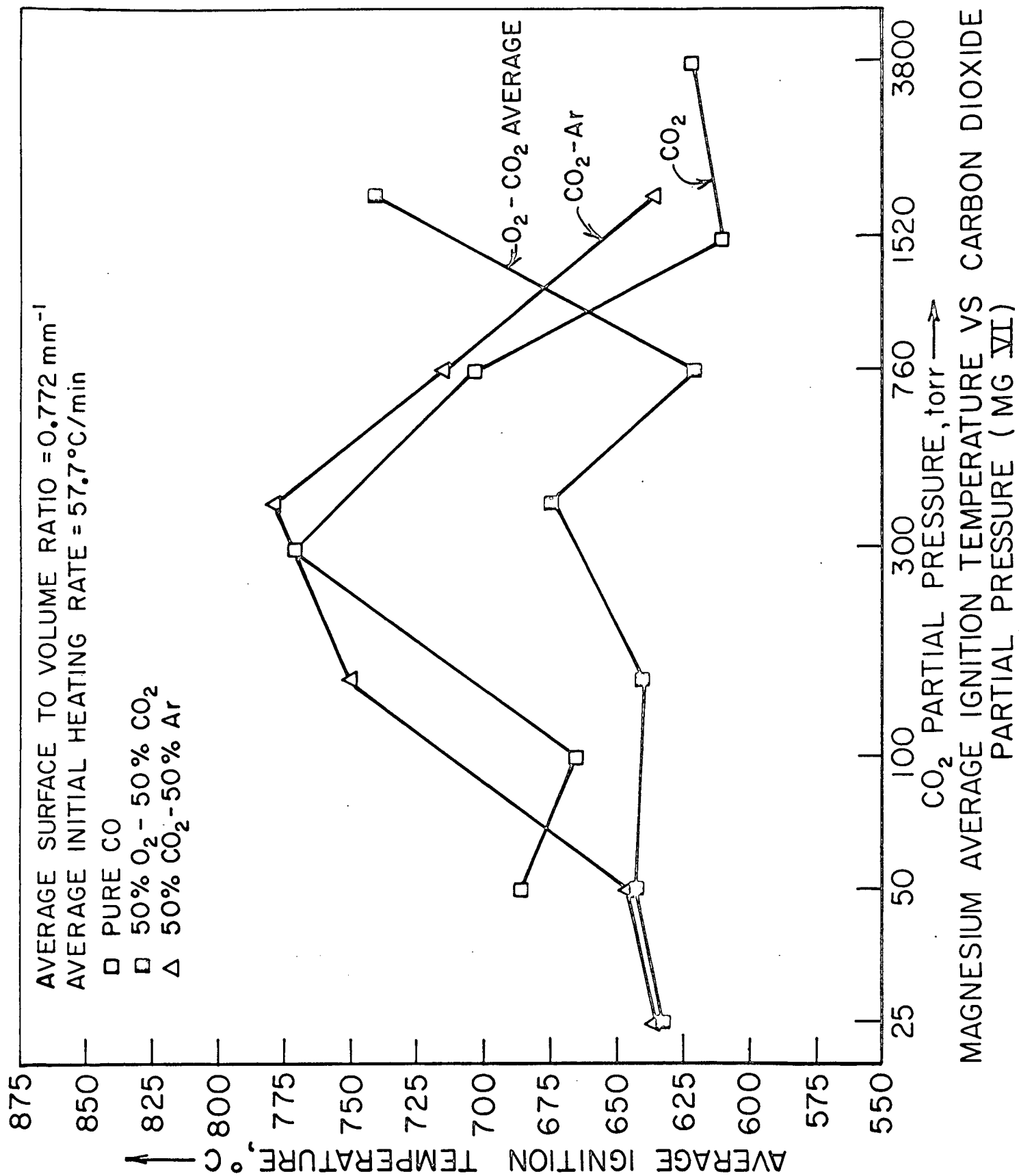


FIGURE 6